

## Digital Redesign of Gust Load Alleviation System using Control Surface

Hyosung Tak\*, Cheolkeun Ha\*

Sang-Wook Lee<sup>+</sup>, Tae-Uk Kim<sup>+</sup>, In-Hee Hwang<sup>+</sup>

\* Department of Aerospace Engineering., University of Ulsan, Korea

(Tel : +82-52-259-2590; E-mail: [cha@mail.ulsan.ac.kr](mailto:cha@mail.ulsan.ac.kr))

<sup>+</sup> Korea Aerospace Research Institute, Korea

(Tel : +82-42-860-2833; E-mail: [lsw@kari.re.kr](mailto:lsw@kari.re.kr))

**Abstract:** This paper deals with the problem of gust load alleviation in active control for the case that aeroelasticity takes place due to interaction between wing structure and aerodynamics on wing when aircraft meets gust during flight. Aeroservoelasticity model includes wing structure modeled in FEM, unsteady aerodynamics in minimum state approximate method, and models of actuator and sensors in state space. Based on this augmented model, digitally redesigned gust load alleviation system is designed in sampled-data control technique. From numerical simulation, this digital control system is effective to gust load on aircraft wing, which is shown in transient responses and PSD analysis to random gust inputs.

**Keywords:** Gust Loads Alleviation, Aeroservoelasticity, LQG design, Optimal Digital Redesign, PSD analysis

### 1. INTRODUCTION

Recently gust load alleviation became one of the important research areas in aircraft design problem. Especially it is important because aircraft wing structure becomes lighter and more flexible as many materials and wing design technology have been developed. In general, gust load influences heavily on aircraft with high aspect ratio wing. If gust attacks such an aircraft wing on which aerodynamics and structural dynamics interact, then deformation and fatigue of the wing structure occur seriously. As this phenomenon continues on the wing structure, finally wing structural damage and destruction might happen. Because of these serious problems, gust load alleviation in wing control surface has been studied to control gust effect on wing and improve aircraft stability and ride quality. In this paper, we studied active control of gust load to alleviate its effect on wing. To do this, first of all, aeroservoelastic wing is modeled. In the modeling process, wing structure is modeled in finite element method, and furthermore unsteady aerodynamics and actuator model are considered as well as gust model. Based on this aeroservoelastic model, an active digital control system for gust load alleviation is designed in optimal control technique in a redesign process considering stability and performance. Finally the gust load alleviation system deigned is evaluated in numerical simulation in the aeroservoelastic model. In section 2, aeroservoelastic model is modeled in details. Then digital redesign process is explained in section 3. Finally the simulation results of the active gust load alleviation system and conclusion are given in section4 and section 5.

### 2. AEROSERVOELASTIC MODEL

#### 2.1 Modeling of Component Models in State Space

In this study, gust load alleviation system consists of wing structural/aerodynamic model, actuator model, gust model as external disturbance source, and feedback control system. The feedback control system is based on acceleration in wing tip and strain in wing root. This overall system is depicted in Fig.1. In the next subsection, the aeroservoelastic model is

explained in details.

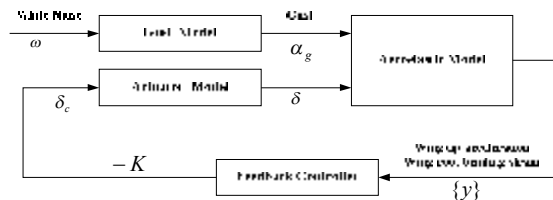


Fig.1 Gust Loads Alleviation System in Feedback Control

#### (1) Aeroelastic Wing Model

For aircraft wing affected by gust, the governing equation of wing aeroelasticity can be expressed in Eq.(1),

$$[M_s]\{\ddot{\zeta}\} + [C_s]\{\dot{\zeta}\} + [K_s]\{\zeta\} = [Q_a]\{\zeta\} + [Q_c]\{\zeta_c\} + [Q_G]\frac{\omega_g}{V} \quad (1)$$

where  $[M_s]$ ,  $[C_s]$ ,  $[K_s]$  are generalized mass, damping, and stiffness matrices, respectively. Also  $[Q_a]$ ,  $[Q_c]$ ,  $[Q_G]$  denote structural vibration modes, unit rotational displacement of control surface, and generalized unsteady aerodynamic matrices, respectively. Moreover  $\{\zeta\}$ ,  $\{\zeta_c\}$ ,  $\omega_g$ ,  $V$  implies generalized coordinates, control signal coming from control surface, gust velocity, and airspeed, respectively. In order to apply the aeroservoelastic model to gust load control problem, Eq.(1) should be expressed in state space. Generalized unsteady aerodynamic matrices ( $[Q_a]$ ,  $[Q_c]$ ,  $[Q_G]$ ), which is calculated in predetermined Mach number and normalized vibration frequency in frequency domain, are required to be approximated in Laplace domain. In this paper, minimum state approximation technique is applied to the aerodynamic matrices. When the minimum state approximation is applied to the generalized aerodynamic matrix  $[Q]$ , defined to be  $[Q] = [Q_a \quad Q_c \quad Q_G]$ , the generalized aerodynamic matrix is expressed in Eq.(2)

$$[\tilde{Q}(s)] = [A_0] + [A_1]s + [A_2]s^2 + [D]([I]s - [R])^{-1}[E]s \quad (2)$$

where  $\bar{s} (= sb/V)$  is defined to be normalized Laplace

variable, and  $b$  is half of the reference chord.  $[R]$  is a diagonal matrix with negative real number, which determines number of aerodynamic state variables. In this paper, diagonal elements of  $[R]$  are selected to be -0.3. Also real matrices of  $[A],[A_1],[A_2],[D],[E]$  are obtained from the aerodynamic matrix  $[Q]$ . Finally, after Eq.(2) is substituted into Eq.(1), the governing equation of aeroservoelasticity model is obtained in state space, which is given in Eq.(3),

$$\{\dot{x}_s\} = [A_s]\{x_s\} + [B_s]\{u_s\} + [B_G]\{\omega_g\} \quad (3)$$

where the related terms of the equation are defined to be

$$\{\omega_s\} = \{\xi, \dot{\xi}, x_a\}^T, \{u_s\} = \{\delta, \dot{\delta}, \ddot{\delta}\}^T, \{\omega_G\} = \{\omega_g, \dot{\omega}_g\}^T$$

and  $x_a$  denotes aerodynamic state variable which comes from approximate of the generalized aerodynamic matrix. Also  $\{u_s\}$  is input vector of control surface, and  $\{\omega_G\}$  is gust input vector.

### (2) Actuator Model of Control Surface

Actuator transfer function of control surface in this wing model is expressed in Eq.(4).

$$\frac{\delta}{\delta_c} = \frac{a_s}{s^3 + a_1s^2 + a_2s + a_3} \quad (4)$$

This model is now described in state space as shown in Eq.(5).

$$\{\dot{x}_c\} = [A_c]\{x_c\} + \{B_c\}\delta_c \quad (5)$$

where the state variable is defined to be  $\{x_c\} = \{\delta, \dot{\delta}, \ddot{\delta}\}^T$ .

### (3) Gust Model

As a gust model, Dryden gust model is used to simulate continuous gust load on wing. The power spectral density of the gust load is described in Eq.(6).

$$\Phi_{\omega_g}(\omega) = \sigma_{\omega_g}^2 \tau_g \frac{1 + 3(\tau_g \omega)^2}{[1 + (\tau_g \omega)^2]^2} \quad (6)$$

Here  $\sigma_{\omega_g}$  denotes root mean square (RMS) of gust velocity, and  $\tau_g = L/V$  where  $L$  is scale of gust turbulence. From Eq.(6), transfer function of gust load can be obtained in spectral decomposition. After a low pass filter  $a/(s+a)$  is applied to the transfer function of Eq.(6), the gust model in state space is obtained in Eq.(7). Note that  $\{y_g\}$  is a vector of  $\{\omega_g, \dot{\omega}_g\}^T$  and  $\omega$  is white noise input.

$$\begin{cases} \{\dot{x}_g\} = [A_g]\{x_g\} + \{B_g\}\omega \\ \{y_g\} = [C_g]\{x_g\} \end{cases} \quad (7)$$

### (4) Aeroservoelasticity Model

Now, augmented aeroservoelasticity model is obtained to design a feedback control in this subsection. This augmented model includes the models given in Eq.(3), Eq.(5) and Eq.(7). First, define the augmented state vector  $\{x\}$  in Eq.(8).

$$\{x\} = \{\xi, \dot{\xi}, x_a, x_c, x_g\}^T = \{x_s : x_c : x_g\}^T \quad (8)$$

where  $x_s : x_c : x_g$  denotes the state variables related with structural vibration modes, actuator modes and gust mode. Then the final form of the aeroservoelasticity model in state space is expressed in Eq.(9),

$$\begin{cases} \{\ddot{x}\} = [A]\{x\} + \{B\}\delta_c + \{D\}\omega \\ \{y\} = [C]\{x\} \end{cases} \quad (9)$$

Here the measured output vector  $\{y\}$  consists of acceleration and strain signals for feedback control, and the associated matrices of  $[A], \{B\}, \{D\}$  have the following expression in Eq.(10),

$$[A] = \begin{bmatrix} [A_s] & [B_s] & \{B_g\} & [C_g] \\ 0 & [A_c] & 0 & 0 \\ 0 & 0 & [A_g] & 0 \end{bmatrix}, \{B\} = \begin{bmatrix} 0 \\ \{B_c\} \\ 0 \end{bmatrix}, \{D\} = \begin{bmatrix} 0 \\ 0 \\ \{B_g\} \end{bmatrix} \quad (10)$$

## 2.2 Verification of Aeroservoelasticity Model

### (1) Analysis of Aeroelasticity Model

In general, simple aircraft wing analytical model is used to design a feedback control system. In this paper, a simple wing model as shown in Fig.2 is used to design a gust load alleviation control system.

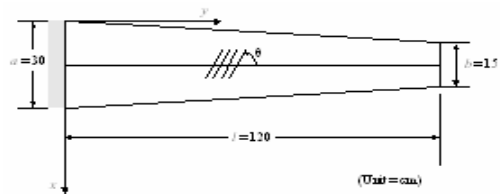


Fig.2 Simplified Aircraft Wing Configuration

Material of the wing structure is Graphite-epoxy composite, and the wing root is fixed as like cantilever beam boundary condition. Also sequence of composite layer is  $[90/\pm 45/0(\text{deg})]$ , thickness of each layer is equally 0.018cm. In order to obtain the aeroservoelasticity model in Eq.(9), natural vibration mode of wing structure and its related generalized aerodynamic matrices in Eq.(2) are precalculated. In this paper MSC/NASTRAN is used to do that and the finite element model of aircraft wing is shown in Eq.(3). The 1<sup>st</sup>~4<sup>th</sup> natural vibration modes are shown in Fig.4. where the 1<sup>st</sup> and 2<sup>nd</sup> bending modes, 2<sup>nd</sup> twist model and 1<sup>st</sup> inplane mode are shown. From analysis of gust load influence on the wing model, it is known that two bending modes and 1<sup>st</sup> twist mode belonging to low frequency range is dominantly influenced by gust turbulence. So those modes are included in the analytic aeroservoelasticity model. The generalized aerodynamic matrices are calculated in the condition of 0.2 Mach number and 21 normalized natural frequencies ( $k=0.001\sim 1.5$ ). The calculated aerodynamic matrices are approximated in

minimum state approximation technique in frequency. For this analytical simple model it is known that inclusion of more than 8 aerodynamic state variables to the model is enough for the approximate error to become steady state. It is shown in Fig.5 that that the approximate generalized aerodynamic state variables based on 8 aerodynamic states are close enough to the results in MSC/NASTRAN.

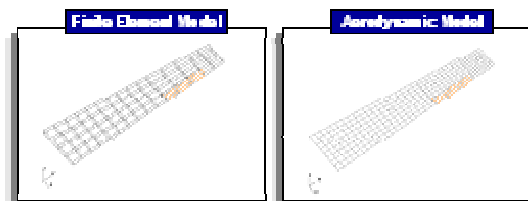


Fig.3 Finite Element and Aerodynamic Model

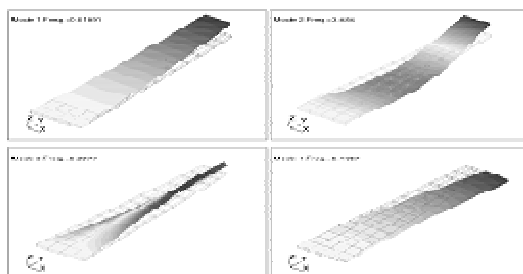


Fig.4 Normal Modes of Simplified Aircraft Wing Model

**(2) Analysis of Continuous Gust**

In this subsection, continuous gust analysis is conducted to compare the result obtained from dynamic aeroelasticity module in NASTRAN and the result yielded from the aeroservoelasticity model shown in Eq.(9). Dryden Power Spectral Density as continuous gust model is used in the condition of air stream velocity of 15m/s, vertical gust velocity of 0.5m/s, and gust scale length of 2m. Note that structural damping ratio is not considered. RMS of displacement, acceleration, and deformation, calculated in NASTRAN and the method given in this study, to continuous gust, are shown in Table 1, where displacement and acceleration are the vertical components in wing tip, and deformation rate is the value of the external upper surface in the wing root.

**Table 1 Comparison of RMS Response (NASTRAN vs. ASE approach)**

Response	NASTRAN	ASE Model	Error(%)
Displacement	9.47	9.67	2.1%
Acceleration	426.65	433.62	1.6%
Strain ( $\epsilon_x$ )	1.06e-4	1.07e-4	0.8%
Strain ( $\epsilon_y$ )	2.64e-3	2.68e-3	1.3%
Strain ( $\gamma_{xy}$ )	5.95e-4	5.90e-4	-0.9%

Note that either case in Table 1 show error within 3%.

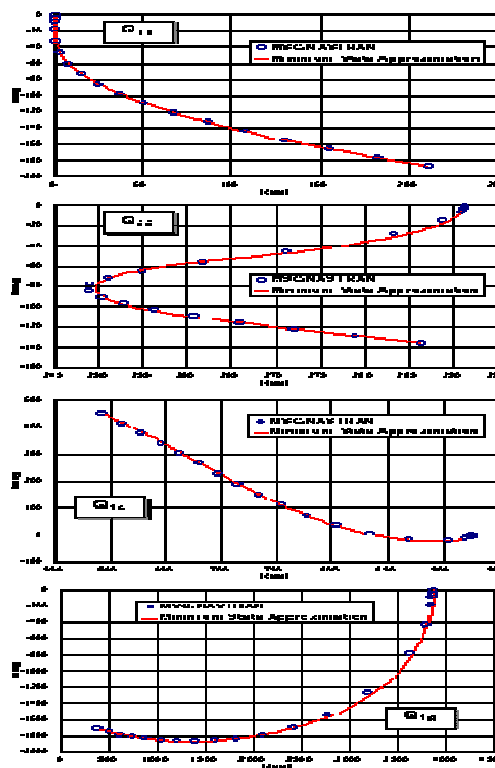


Fig.5 Minimum State Approximation Results for Generalized Aerodynamic Matrices

**2.2 Active Control System for Gust Load Alleviation**

Now, active control system for gust load alleviation is designed in output feedback of the aeroservoelasticity model given in Eq.(9). Control technique in this paper is based on Linear Quadratic Gaussian(LQG). To be an effective control system to gust turbulence, Frequency Shaped LQG technique is applied to this problem. This technique has a merit that appropriate frequency shaping can protect some structural modes sensitive to gust turbulence. Once an active control system in continuous-time domain is designed and its performance is evaluated, which will be good enough, the control system is optimally redesigned. Therefore final goal of our control system design is to design an appropriate digital control system, which is optimally redesigned and considering inter-sample response to gust turbulence.

**(1) Performance Index**

In optimal control design, a proper performance index is important because optimality is solely based on the performance index defined. Here we define a performance index given in Eq.(11), which is the frequency shaped quadratic form,

$$J = \frac{1}{2} \int_{-\infty}^{\infty} (\{z(j\omega)\}^T [Q(j\omega)] \{z(j\omega)\} + \{\delta_{ec}(j\omega)\}^T \{\delta_{ec}(j\omega)\}) d\omega \quad (11)$$

where  $\{z(j\omega)\}$  is performance criterion vector, which is the same as system measurement outputs  $\{y\}$ , and  $\{\delta_{ec}(j\omega)\}$  denotes  $\delta_c$ . Also  $\{Q(j\omega)\}$  is a frequency shaping filter,

which is designed in consideration of gust turbulence PSD. In this design, this filter design is very important to get a good performance of gust load alleviation, where the structure in state space is defined in Eq.(12),

$$[Q(s)] = \begin{cases} \dot{x}_q = [A_q]x_q + [B_q]\xi_q \\ y_q = [C_q]x_q + [D_q]\xi_q \end{cases} \quad (12)$$

Once the frequency shaping filter  $\{Q(s)\}$  is designed, the state variable in Eq.(12) is augmented to Eq.(9) and then rewrite the state equations and performance index in Eq.(12),

$$\begin{aligned} \dot{x}_e &= [A_e]x_e + [B_e]\delta_e + [D_e]\omega \\ y_e &= [C_e]x_e + v \\ J &= \frac{1}{2}E\{x_e\}^T [Q_e]x_e + \delta_c^2 \end{aligned} \quad (13)$$

where  $\{x_e\}^T = \{x_e\}^T \{x_q\}^T$ , and the related matrices are defined to be,

$$\begin{aligned} [A_e] &= \begin{bmatrix} [A] & [0] \\ [B_q][C] & [A_q] \end{bmatrix}, \{B_e\} = \begin{Bmatrix} \{B\} \\ \{0\} \end{Bmatrix} \\ [C_e] &= [[D_q] \quad [C] \quad [C_q]], \{D_e\} = \begin{Bmatrix} \{D\} \\ \{0\} \end{Bmatrix} \\ [Q_e] &= \begin{bmatrix} [C]^T [D_q]^T [D_q][C] & [C]^T [D_q]^T [C_q] \\ [C_q]^T [D_q][C] & [C_q]^T [C_q] \end{bmatrix} \end{aligned} \quad (14)$$

To the formulation shown in Eq.(13), LQG design technique would be applied. However this approach might not get a good design result. So in this paper LQG/LTR approach is utilized to design an optimal compensator, where LTR process is applied to optimal Kalman estimator design. After trial and error many times, we could have a good analog controller. What to do next is how to redesign an optimal digital controller, which has closed-loop stability and performance as good as those of the analog optimal controller (LQG/LTR compensator). It is mentioned that in the digital design, intersample response to gust should be able to be considered in the design process.

### 3. DIGITAL REDESIGN IN OPTIMAL CONTROL SETTING

#### 3.1 Optimal Sampled-Data Control Design

In this paper we propose a setting of sampled-data control design shown in Fig.6. Here we assume that sampling time (h) is predetermined, and ideal sampler(S) and zero-order-hold (ZOH) is adopted. Also  $K_d$  in Fig.6 is a digital controller.

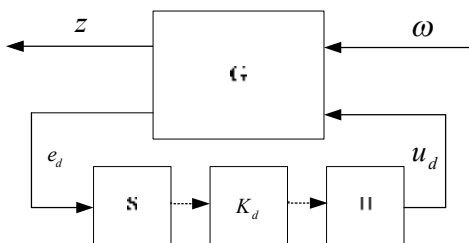


Fig.6 Setting of Sampled-data Control System

The augmented plant (G), given in Eq.(13), is redefined to be

$$G(s) = \begin{bmatrix} A & B_1 & B_2 \\ C_1 & D_{11} & D_{12} \\ C_2 & D_{21} & 0 \end{bmatrix} \quad (15)$$

Once all the data are set in Eq.(13) and Eq.(15), ZOH equivalent transformation is applied to Eq.(13) and Eq.(15). The result of the transformation is shown in Fig.6, where the equivalent plant ( $G_d$ ) is defined to be,

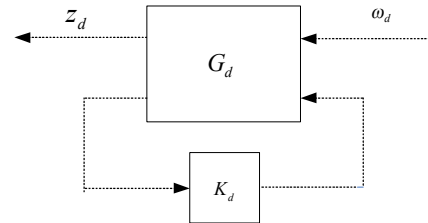


Fig.7 Discrete-time Generalized Sampled-data Setup

$$G_d(z) = \begin{bmatrix} A_d & B_{1d} & B_{2d} \\ C_{1d} & D_{11d} & D_{12d} \\ C_2 & D_{21} & 0 \end{bmatrix} \quad (16)$$

Note that the associated matrices in Eq.(16) are defined to be,

$$A_d = e^{hA}, [B_{1d} \quad B_{2d}] = \int_0^h e^{A\tau} d\tau [B_1 \quad B_2] \quad (17)$$

$$[C_{1d} \quad D_{11d} \quad D_{12d}]' [C_{1d} \quad D_{11d} \quad D_{12d}] = M$$

where the matrix M is factorized in cholsky factorization, which is obtained from the integral of

$$\begin{aligned} M &= \int_0^h e^{\tau A'} [C_1 \quad D_{11} \quad D_{12}]' [C_1 \quad D_{11} \quad D_{12}] e^{\tau A} d\tau \\ A &= \begin{bmatrix} A & B_1 & B_2 \\ 0 & 0 & 0 \end{bmatrix} \end{aligned}$$

Also the performance index J in Eq.(13) is discretized, in which inter-sample information is included, shown in Eq.(18)

$$J_d = \frac{1}{2}E[Z_d^T Z_d] \quad (18)$$

Now, this problem is solved in discrete-time  $H_2$  optimal control. The solution technique are given in Ref.[7]. The optimally redesigned control system for the gust load alleviation is given to be,

$$\begin{aligned} x_{k+1}^c &= A_c x_k^c + B_c y_k \\ u_k &= C_c x_k^c + D_c y_k \end{aligned} \quad (19)$$

Note that the digital controller in Eq.(19) has order equal to order of the plant in eq.(16).

### 4. NUMRICAL SIMULATION

#### 4.1 Evaluation of Gust Load Alleviation Design

So far we proposed a digital redesign technique set up in optimal control framework. In the design process, inter-sample response to gust is considered. In this paper, the augmented system is of 23<sup>rd</sup> order and one control input and two sensor outputs. It is noted that the optimal discrete-time controller for gust load alleviation consists of the compensator (23<sup>rd</sup> order)

in Eq.(19) and the filter (2<sup>nd</sup> order) in Eq.(12). The simulation results of transient time responses are shown in Fig.8. From this figure, DLQG gust load alleviation (GLA) is more effective to gust than LQG GLA for both of strain and acceleration. Also from Fig.9, since the aircraft wing is sensitive to gust within 4Hz, GLAs of DLQG and LQG system designed are strongly effective to this gust. It is observed from PSD in Fig.9 that the GLA in DLQG system is at least similar to that in LQG system. This implies that digital redesign technique proposed in this paper works well. Also, we know from Fig.8 and Fig.9 that gust load response is degraded to be worse if GLA is off.

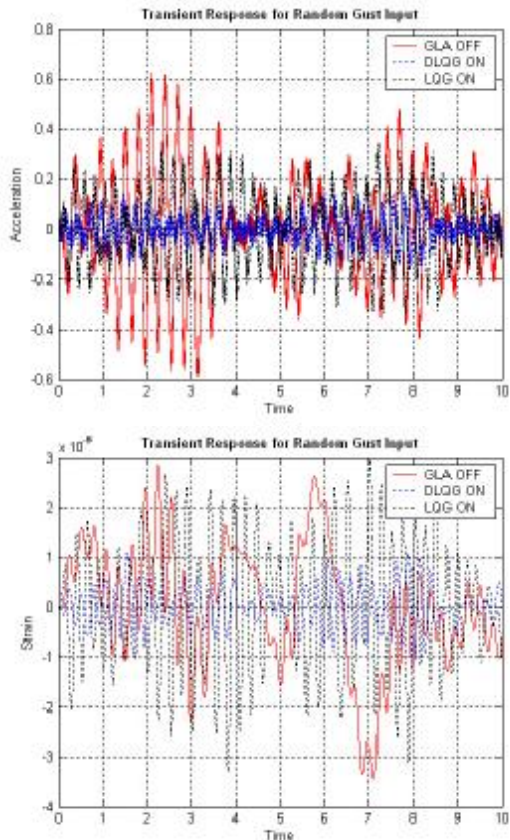


Fig.8 Transient Response for Random Gust Input

**4. CONCLUSION**

So far we considered gust load alleviation problem in active control and digital redesign of GLA system for practical implementation to aircraft. The proposed DLQG design is effective to gust load alleviation for the wing designed, which is shown in numerical simulation results in this paper.

**Acknowledgement**

This research is parts of the results from “Development of Core Technology for UAV Performance/Control/Safety Enhancement” project which is supported by KORP(Korea Research of Public Science & Technology) and is performed by KARI(Korea Aerospace Research Institute).

**REFERENCE**

- 1) Karpel, M., "Design for Active Flutter Suppression and Gust Alleviation Using State-Space Aeroelastic Modeling," *Journal of Aircraft*, Vol.19, 1982, pp.221-227
- 2) Karpel, M., "Time-Domain Aeroservoelastic Modeling Using Weighted Unsteady Aerodynamic Forces," *Journal of Guidance and Control*, Vol.13, No.1, 1990, pp.30-37
- 3)Hoadley, S. T. and Karpel, M., "Application of Aeroservoelastic Modeling Using Minimum State Unsteady Aerodynamic Approximations," *Journal of Guidance and Control*, Vol.14, No.2, 1991, pp.1267-1276.
- 4) Baldelli, D. H., Ohta, H. and Nitta K., "Gust Load Alleviation of an Aeroelastic Wing Model," *Transactions of the Japan Society for Aeronautical and Space Sciences*, Vol.36, No.113, 1993, pp.125-142
- 5)Rodden, W. P. and Johnson, E. H., *MSC/NASTRAN Aeroelastic Analysis User's Guide, V68*, MSC, 1994.
- 6) Reymond M., *MSC/NASTRAN 2001 DMAP Programmer's Guide*, MSC, 2000
- 7) Tongwen Chen and Bruce Francis, “Optimal Sampled-Data Control Systems” *Springer*, 1995
- 8) Bunjamin C. Kuo “Digital Control System”, *Oxford Univ. Pr* 1997, pp434-454

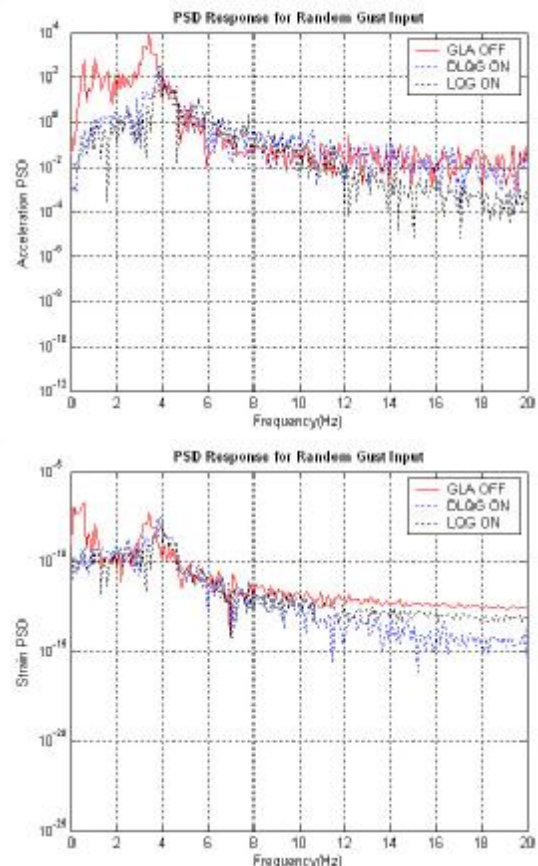


Fig.9 PSD Response for Random Gust Input